Uncovering the Neural Code Using a Rat Model during a Learning Control Task

Chenhui Yang, Hongwei Mao, Yuan Yuan, Bing Cheng, and Jennie Si

Arizona State University, Tempe AZ 85287, USA

Abstract. How neuronal firing activities encode meaningful behavior is an ultimate challenge to neuroscientists. To make the problem tractable, we use a rat model to elucidate how an ensemble of single neuron firing events leads to conscious, goal-directed movement and control. This study discusses findings based on single unit, multi-channel simultaneous recordings from rats frontal areas while they learned to perform a decision and control task. To study neural firing activities, first and foremost we needed to identify single unit firing action potentials, or perform spike sorting prior to any analysis on the ensemble of neural activities. After that, we studied cortical neural firing rates to characterize their changes as rats learned a directional paddle control task. Single units from the rat's frontal areas were inspected for their possible encoding mechanism of directional and sequential movement parameters. Our results entail both high level statistical snapshots of the neural data and more detailed neuronal roles in relation to rat's learning control behavior.

1 Introduction

The neural events leading to a voluntary movement, or an intentional purposeful movement, may be characterized by three complex processes: target identification, plan of action, and execution. Several distinct regions of the cerebral cortex are believed to be involved in governing these processes, including the posterior parietal cortex, the premotor areas (PM) of the frontal cortex, and the primary motor cortex (M1) [Kandel et al. (2000)]. Adaptation represented in neural firing events has been observed in motor cortical areas which correlate with improved behavioral parameters [Kargo et al. (2004)]. Premotor and parietal areas appear to participate in a fundamental event necessary to purposeful movement: the translation of sensory inputs into motor coordinates needed to specify precise movements [Andersen et al. (2004)]. On the other hand, there has been growing evidence of M1's involvement in sequential tasks using a monkey model [Ben-Shaul et al. (2004); Carpenter et al. (2004); Kakei et al. (1999); Li et al. (1999); Lu et al. (1999); Shima et al. (2000)]. The study in [Shima et al. (2000)] showed that supplementary (SMA) played roles in task execution but presupplementary (pre-SMA) area was responsible for learning new aspects of a task in memorized tasks. In a rat model, existing studies were based on short-duration behavioral tasks (e.g. 20ms). However, there is little anatomical or functional evidence that rats have a well delineated pre-SMA.

Even though the frontal areas of a rat is not as elaborate as a primate, it is however well observed, including our own data, that rats do have the capability to derive abstract

J. Liu et al. (Eds.): WCCI 2012 Plenary/Invited Lectures, LNCS 7311, pp. 261–279, 2012.

control strategy via associative learning. Therefore, in this study, we aim to perform a functional study to examine neural coding in the primary motor cortex (M1) and the premotor cortex (PM) during a rat's natural movement in response to a cognitive control task that requires multiple presses at a control paddle. This study centers on investigating the following three aspects. First, neural adaptation may be reflected in the mean firing rate of a motor cortical neural ensemble during learning of a cognitive control task. Second, a larger percentage of PM neurons may be involved in interpreting sensory stimuli and motor planning than M1 neurons. Third, M1 neuronal responses vary according to the movement context in a multiple press task.

In the following, we first introduce an automated action potential detection algorithm which is an important first step to perform any analysis on single unit based analysis of neuronal firing activities. Spike rate based analyses will then be carried out using the sorted single unit spikes. The aims of the analyses are to characterize the rat's behavioral learning parameters by providing a neural substrate based on simultaneously recorded multiple neurons in the rat's motor cortical areas.

2 Single Unit Recording from Behaving Rats

In this section we provide details of our experimental set up, from behavioral training to simultaneous electrophysiolocal recording of single unit neural activities from an ensemble of neurons in the rat's motor cortical areas.

2.1 Animal Handling and Training Procedures

All procedures involving animals were conducted according to the National Guidelines on Animal Experiments and were approved by the Arizona State University Institutional Animal Care and Use Committee.

Recording electrode implant surgeries were performed when the rats reached a weight of 390-500 grams and they were proficient (with an accuracy of 90% or higher) at pressing the control paddle inside the Skinner training chamber for at least 3 consecutive days. Once recording began, rats were food restricted to a daily diet of 12-15 grams of food pellets including the amount of reward collected during the recording session. Food restricted rats were monitored for their weights to be above 80% of the average weight at their respective age.

2.2 Surgical Procedures

Figure 1(a) illustrates the craniotomy for the electrode array to be placed. Additionally, 3 anchor holes were drilled between bregma and lambda: 2 in the right hemisphere and 1 in the left hemisphere, for mounting bone screws which serve as signal ground and also provide fixation to secure the head cap. A 16 channel microwire array (Omnetics or ZIF-Clip, TDT Corporate, Florida) was then lowered slowly into the craniotomy while neural signals were monitored in real time. The target depth was about 1.8-2.3 mm from dura aiming for layer 5 pyramidal neurons. The final depth was determined by optimal spiking activities on majority of the recording channels.

2.3 Electrophysiology

Neural waveforms were recorded through 16-channel microwire arrays connected with an omnetics headstage or a Zif-clip headstage by TDT (Medusa Connector LP16CH or ZIF-Clip ZC16). Analog waveforms passed through a unity gain preamplifier (Medusa PreAmp RA16PA, TDT Corporate), which also provides a band-pass filter (2.2 Hz to 7.5 kHz). The waveforms were digitally sampled at 24414 Hz and then sent over a fiber optic link to a DSP device, where they were filtered (band-pass 300 Hz to 3 kHz), and processed (cross channel denoising) in real-time (RX5/RX7, TDT Corporate). The stored waveforms were spike sorted offline into single unit action potentials using a multi-scale correlation of wavelet coefficients (MCWC) spike detection algorithm [Yang et al. (2011)] followed by a template matching sorting procedure. Events in the behavioral task such as cue on, paddle release, paddle press and food reward were registered simultaneously and time stamped by the TDT system.

2.4 Behavioral Task

Rats were freely moving inside a Skinner box when not performing the designed task. The task is self-paced, which is for the rat to associate light cues with control paddles. The chamber is dark with a 0.5 watt infrared light illumination for video recording. Figure 1(b) is a top view of the recording chamber. When working on the task, the rat faced the front panel of the chamber where 5 red LED lights were placed. At most one cue light was lit at any given time. The 3 control paddles were to be used by the rat to

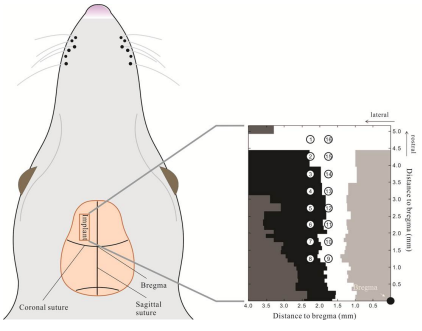

(a) Implant site: a 16-channel array was placed in the frontal area of the rat with the center at 3 mm anterior and 2 mm lateral from bregma. Numbered circles indicate electrode positions. Black area is the primary cortex, and white area is the secondary motor cortex, according to the rat brain atlas.

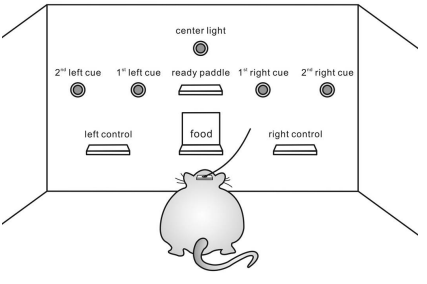

(b) The recording chamber. The rat pressed the center paddle to signal the start of a new trial. As one of the cue light appeared, the rat had to make a decision of pressing either the left or right control paddle to control the movement of the light. Each left/right press of the control paddle moved the light in the right/left direction by one step.

Fig. 1. Experimental setup

complete the association task. A center control paddle was placed for the rat to press as a signal of a new trial start. The two control paddles on each side of the central paddle were for controlling the movement of the light positions. A food pellet dispenser was located in the center paddle for rewarding the rat. The goal of the task was to move the light position to the center by pressing the control paddles and remain there for 1 second. The rat was not able to start a new trial until a lapse of 8 seconds for successful trials and 15 seconds for failed or timed-out trials, respectively. Upon pressing of the center paddle by the rat to start a new trial, one of the 5 cue lights was lit. Two seconds later, both control paddles were released. Right paddle moved the light to the left by one light position and similarly for the right side. The rats were naive initially and they learned the task by trial and error. If they managed to keep the light remain in the center position for 1 second, they would be rewarded with food pellets. If the rats did not respond by pressing any paddle within the time allowance of 1 second or if the light moved out of range, the trial was deemed a failure.

3 Spike Detection Based on Wavelet Transform

Extracellular chronic recordings have been used as important evidence in neuroscientific studies to unveil the fundamental neural network mechanisms in the brain. Spike detection is the very first step in the analysis of the recorded neural waveforms to decipher useful information and to provide useful signals for brain machine interface applications. This multiscale correlation of wavelet coefficients (MCWC) is an automated spike detection algorithm, which leverages a technique from wavelet based image edge detection. It utilizes the correlation between wavelet coefficients at different sampling scales to create a robust spike detector. The algorithm has one tuning parameter, which potentially reduces subjectivity of detection results. Compared with other detection algorithms, the proposed method has a comparable or better detection performance.

3.1 Introduction to Spike Detection

Neural action potentials, also known as nerve impulses or spikes, play an important role in understanding the central nervous system. In chronic multichannel recordings from behaving animals, action potentials are obtained by multichannel electrodes implanted in brain areas of interest. As such, noise from brain tissues, muscle movement, and other biological and instrumental interferences are inevitable [Musial et al. (2002)]. As the first step of neuroscientific studies and engineering applications such as brain machine interfaces, identifying real neural spikes from noisy recordings is essential.

The wavelet transform is a technique for representing a time domain signal by a set of functions that are scaled and time-translated from a mother wavelet. Its characteristics make it a natural candidate for transient signal representation and thus spike detection applications. Several spike detection algorithms based on wavelet transforms have been proposed [Yang et al. (1988),Kim et al. (2003),Hulat et al. (2000),Hulat et al. (2002),Quiroga et al. (2004),Oweiss et al. (2002a), Oweiss et al. (2002b),Nenadic et al. (2005), Benitez et al. (2008)].

It is noticed that simple threshold based detection methods are intuitive in principle and easy to implement. This is echoed by its popularity including commercial realizations of the algorithms. However as pointed out in [Wood et al. (2004)], the detection results are variable and subjective to users, in addition to high false alarm rates. Other than these direct thresholding of the recorded neural waveforms as a function of time, the idea of thresholding was also an important part of several other approaches, such as the threshold applied to wavelet coefficients in [Yang et al. (1988)] and [Kim et al. (2003)], a higher than usual threshold to gather spikes as the ground truth in [Song et al. (2006)], the threshold applied to the output of minimum average correlation energy (MACE) filter in [Dedual et al. (2007)], the threshold for selecting potential neural spikes in [Hulat et al. (2002)] and [Hulat et al. (2000)], two thresholds used in multiresolution generalized likelihood ratio test (MRGLRT) in [Oweiss et al. (2002a)] and [Oweiss et al. (2002b)], and the threshold used for separating neural spikes from noise in [Nenadic et al. (2005)]. It is worth pointing out that several algorithms rely on a Gaussian noise assumption to make an optimal detection statement. On one hand, it gives users some assurance of optimality, but unfortunately, noise profile is rarely Gaussian in recorded neural waveforms.

The MCWC aims at providing robust detection performance with high detection rate and low false alarm. The goal is to alleviate subjectivity and variability in detection results. In doing so, we made use of the observation that a sharp rise of neural waveform signifying the onset of a neural spike in a 1-D neural signal is similar in characteristic to an edge in a 2-D image. Therefore, the MCWC algorithm is a wavelet based approach, inspired by image edge detection. In [Xu et al. (1994)], an edge detection algorithm makes use of a property in wavelet transform coefficients that the wavelet transform coefficients of image edges usually have higher magnitudes than the coefficients from noise. As shown later in this study, the wavelet coefficient magnitudes of neural recordings preserve similar properties with a properly selected wavelet function: coefficients of neural spikes have higher magnitudes than those coefficients of noise.

The MCWC utilizes continuous wavelet transform as that in wavelet detection method (WDM) [Nenadic et al. (2005)] and [Benitez et al. (2008)], however with different wavelet functions in the respective implementations. Another major difference between the two algorithms is that while WDM performs detection at individual wavelet scales prior to fusing the results from multiple levels for a final spike detection, our approach fuses wavelet transforms from multiple scales first at each scale level and then perform a single detection by hypothesis testing. We only introduce one free parameter, which in turn helps reduce the subjectivity of the algorithm.

3.2 Working Principle of the Multiscale Correlation of Wavelet Coefficients (MCWC)

We chose wavelet function “coiflets” based on the following considerations. When the time support of the wavelet function matches the duration of a neural waveform, the corresponding wavelet transform coefficients become high. But the waveforms of noise usually do not resemble the wavelet function. Therefore the coefficients from noise have small or close to zero magnitudes. By inspecting waveforms corresponding to high wavelet transform coefficients, we can detect neural spikes.

The MCWC spike detection algorithm is based on continuous wavelet transform. It takes a multiscale approach by first calculating the wavelet coefficients at each scale, and correlates (by multiplication) wavelet coefficients from multiple scales, and then perform a hypothesis test for spike detection. It is motivated by a robust image edge detection algorithm [Xu et al. (1994)] where in this case, a sharp spike is considered a 1-D edge. What follows is a step by step development of the MCWC algorithm.

3.2.1 Computing Normalized Correlation of Wavelet Coefficients. Consider a neural waveform $x(t)$. Let J be the width of the observation window of the waveform under consideration which is used as the integration interval in the calculation of wavelet coefficients. And let N be the number of samples in the observation window J. With scale factor $\{a_i\} = \{0.5, 0.6, \cdots, 1.5ms\}$, and time translation $\{b_j\} = \{0, 1, 2, \cdots, N-1\}$, we obtain

$$Tx(a_i, b_j) = \int_J x(t) \frac{1}{\sqrt{a_i}} \psi(\frac{t - b_j}{a_i}) dt. \tag{1}$$

$$r_S(a_i, b_j) = \prod_{k=0}^{S-1} Tx(a_{i+k}, b_j). \tag{2}$$

$$P_{r_S}(a_i) = \sum_{j \in J} r_S(a_i, b_j)^2, \tag{3}$$

$$P_{Tx}(a_i) = \sum_{j \in J} Tx(a_i, b_j)^2, \tag{4}$$

$$r'_S(a_i, b_j) = r_S(a_i, b_j) \times \sqrt{\frac{P_{Tx}(a_i)}{P_{r_S}(a_i)}}. \tag{5}$$

Where $\psi(t)$ is wavelet function, $Tx(a, b)$ denotes the wavelet transform of $x(t)$, S is the number of sampling scales in a continuous wavelet transform.

3.2.2 Spike Detection Using Hypothesis Testing.
H_0: $x(t)$ contains no spikes in the small window $[t_0, t_1]$ belonging to J under consideration (Fig. 2),

H_1: $x(t)$ contains a spike at b_j in the small window $[t_0, t_1]$ belonging to J under consideration (Fig. 2).

Specifically, H_0 holds, or no spike is detected if

$$\left| \frac{r'_S(a_i, b_j)}{Tx(a_i, b_j)} \right| \leq 1 \tag{6}$$

and H_1 holds, or a spike is detected if (7) is satisfied,

$$\left| \frac{r'_S(a_i, b_j)}{Tx(a_i, b_j)} \right| > 1 \tag{7}$$

Fig. 3 illustrates the principle of spike detection proposed in this study.

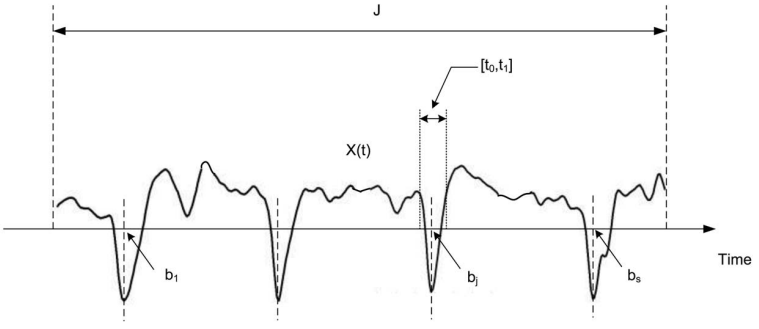

Fig. 2. The integration window for computing wavelet coefficients and illustration of finding spike instants: b_j, $j = 1, 2, \cdots, s$, represent the instants of neural spike peaks

Let H_1 hold inside the small interval $[t_0, t_1]$ at specific points of b_j where there can possibly be more than one b_j's. Let t_d be the instant of a spike within $[t_0, t_1]$ (refer to Fig. 3). Then a spike is detected at t_d within $[t_0, t_1]$ from the following

$$t_d = \underset{\substack{b_j \in [t_0, t_1] \\ a_i \in \{0.5, \cdots, 1.5\}}}{\arg\max} |Tx(a_i, b_j)| \,. \tag{8}$$

The width of the spike detected at t_d, τ, is estimated by

$$\tau = \underset{a_i \in \{0.5, \cdots, 1.5\}}{\arg\max} |Tx(a_i, t_d)| \,. \tag{9}$$

This effectively implies that no other spikes exist within a distance of τ from t_d.

3.2.3 Detection Principle: Adaptive Thresholding. We are now ready to demonstrate that the MCWC detection algorithm actually is an adaptive thresholding method. The threshold level changes as the signal-to-noise ratio or the noise covariance varies.

First, consider the case of $S = 2$. Re-write (7) into the following by assuming that $Tx(a_i, b_j)$ is non-zero, which is commonly true.

$$\left| Tx(a_i, b_j) Tx(a_{i+1}, b_j) \sqrt{\frac{\sum_{j \in J} Tx(a_i, b_j)^2}{\sum_{j \in J} Tx(a_i, b_j)^2 Tx(a_{i+1}, b_j)^2}} \right| > |Tx(a_i, b_j)|. \tag{10}$$

Define $\overline{T}x(a_i, S)|_{S=2}$ as in (11),

$$\overline{T}x(a_i, S)|_{S=2} \triangleq \frac{\sum_{j \in J} Tx(a_i, b_j)^2 Tx(a_{i+1}, b_j)^2}{\sum_{j \in J} Tx(a_i, b_j)^2}. \tag{11}$$

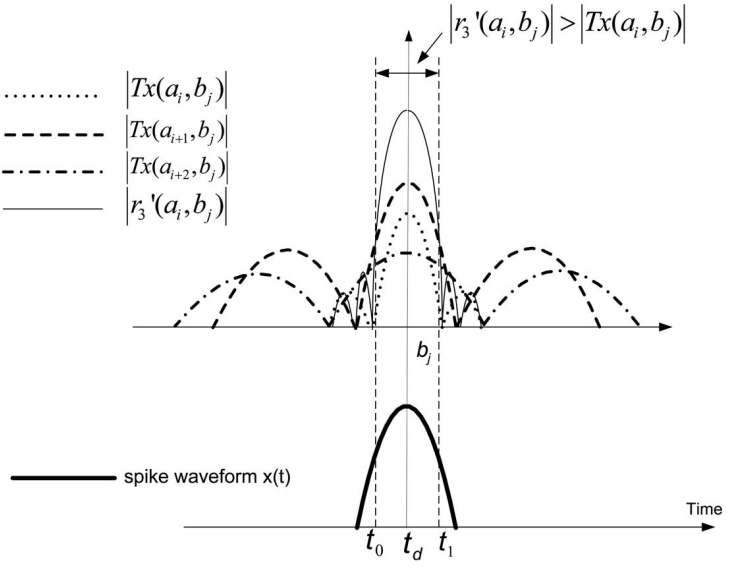

Fig. 3. Demonstration of MCWC detection principle: The multiplication of multi-scale wavelet coefficients enhances the detection of a neural spike. Inequality $|r'_S(a_i, b_j)| > |Tx(a_i, b_j)|_{S=3}$ for $t \in [t_0, t_1]$ indicates that hypothesis H_1 passes the test in this interval. The detection of a neural spike at time instant t_d is declared.

Re-arranging (10) by substituting the newly defined term $\overline{T}x(a_i, S)|_{S=2}$, we obtain the following new form of spike detection criterion,

$$Tx(a_{i+1}, b_j)^2 > \overline{T}x(a_i, S)|_{S=2}. \tag{12}$$

Under a similar assumption to that in [Nenadic et al. (2005)] at the i^{th} scale level, $\{Tx(a_i, b_j)\}$ are independent Gaussian random variables and comply with the following distributions,

$Tx(a_i, b_j) \sim N(0, \sigma^2)$ given H_0 holds, which implies that given H_0, $Tx(a_i, b_j)$ complies with a Gaussian distribution with zero mean and σ^2 as its variance.

$Tx(a_i, b_j) \sim N(\mu, \sigma^2)$ given H_1 holds, which implies that given H_1, $Tx(a_i, b_j)$ complies with a Gaussian distribution with μ as its mean and σ^2 as its variance.

Define a weighting coefficient w_i as shown below,

$$w_i \triangleq \frac{Tx(a_i, b_j)^2}{\sum_{j \in J} Tx(a_i, b_j)^2} = \frac{Tx(a_i, b_j)^2/\sigma^2}{\sum_{j \in J} \left[Tx(a_i, b_j)^2/\sigma^2\right]}. \tag{13}$$

Let $P(H_0)$ be the prior probability associated with hypothesis H_0 and $P(H_1)$ be that with hypothesis H_1. Then for real neural recordings, it is reasonable to assume that $P(H_0) \gg P(H_1)$ since majority of the time course of a neural recording corresponds with noise [Nenadic et al. (2005)]. Given that H_0 holds, then $Tx(a_i, b_j)$ complies with

$N(0, \sigma^2)$. Consequently the new variable $Tx(a_i, b_j)^2/\sigma^2$ complies with the chi-square distribution with 1 degree of freedom, i.e., $Tx(a_i, b_j)^2/\sigma^2 \sim \chi_1^2(1)$. Therefore $E\left[Tx(a_i, b_j)^2/\sigma^2\right] = 1$ remains valid most of the time. It also is approximately true if H_1 holds but the mean μ in $Tx(a_i, b_j)$ is relatively low. Since $E\left[Tx(a_i, b_j)^2/\sigma^2\right] \approx 1$, then $\sum_{j\in J}\left[Tx(a_i, b_j)^2/\sigma^2\right] \approx M$, where M is the cardinalities of J. Thus the weight $w_i \approx 1/M$.

Since $Tx(a_i, b_j)$ for a given scale may be viewed as an independent Gaussian variable with zero mean most of the time especially when it corresponds with noise, the maximum likelihood estimate of the variance of the noise sequence $\{Tx(a_{i+1}, b_j)\}$ is $\frac{1}{M}\sum_J Tx(a_{i+1}, b_j)^2$. To see that, refer to (13) and that $w_i \approx 1/M$. Therefore the threshold $\overline{T}x(a_i, S)|_{S=2}$ defined in (12) can be viewed as an approximation of the maximum likelihood estimation of the noise variance since $P(H_0) \gg P(H_1)$. When $Tx(a_{i+1}, b_j)^2 > \overline{T}x(a_i, S)|_{S=2}$, it implies that the correlation between the neural waveform and the wavelet is greater than the noise variance, and therefore, a neural spike is likely to be present, and that H_1 is true. For $S \geq 3$ case, readers are referred to [Yang et al. (2011)].

Fig. 4(a) and Fig. 4(b) illustrate how the adaptive threshold values vary as a function of the SNR or the noise co-variance and the scale level S.

3.3 Detection Performance Evaluation

In this section, we provide detailed performance evaluation on the multiscale correlation of wavelet coefficient (MCWC) algorithm. While comparisons are conducted for a few algorithms including direct thresholding, our focus is on comparing MCWC and WDM

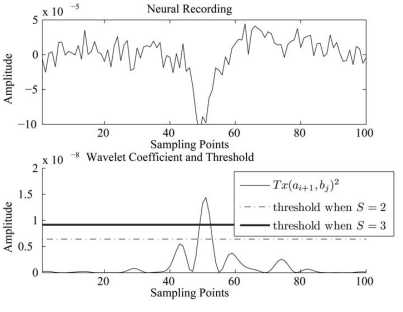

(a) Detection thresholds at two S levels when neural signal has a low SNR or high noise covariance

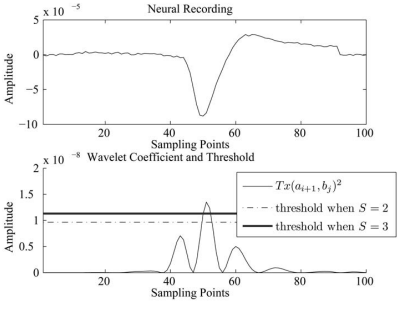

(b) Detection thresholds at two S levels when neural signal has a high SNR or low noise covariance

Fig. 4. Illustration of adaptive threshold in MCWC, which varies with SNRs or noise covariances and S values. From (a) and (b), at a given SNR, when S is high, the threshold levels are high and vice versa. The SNR in (a) is lower than that in (b), therefore at a given S, the threshold level is higher when SNR is higher.

since both are wavelet based, and WDM has been shown outperforming several other approaches [Nenadic et al. (2005)] and [Santaniello et al. (2008)].

18 artificially generated neural waveforms span 50 seconds, and they are sampled at 20KHz. Half of the 18 artificial data sets (A1-1 to A1-9) were obtained with 1dB signal-to-noise ratio (SNR), while the other half (A2-1 to A2-9) with 10dB SNR.

Each artificial neural data set was generated the same way as in [Smith (2006)].

When applying the WDM algorithm, one is required to select a parameter L that determines the cost ratio between the false alarms and missed detections.

3.3.1 Comparison of Detection Performance among Thresholding, MCWC, and WDM Using Artificial Neural Data Sets

In this section, we compare detection performances among MCWC, WDM, and thresholding provided in Plexon's Offline Sorter. Eighteen artificial data sets, A1-1 to A1-9, and A2-1 to A2-9 are used. The thresholding method used was the "Signal Energy" in Offline Sorter as described below,

$$energy(i) = \frac{1}{W} \sum_{j=i-W/2}^{i+W/2} v^2(j), \tag{14}$$

where $v(j)$ is the raw neural recording at time j. W is the window width used in averaging. In this study, $W = 7$ is used.

To make results comparable, we manually selected the threshold value in Offline Sorter such that the total number of detected neural spikes was close to that of the ground truth. The L and S parameters in WDM and MCWC, respectively, were chosen similarly such that the total number of detected spikes by each algorithm was close to the ground truth. To remove low frequency noise, the artificial data sets used in thresholding detection were filtered with a band-pass butterworth filter, which usually enhances its performance. The pass band is [100, 6000]Hz. However, the data used in WDM and MCWC were not filtered. The receiver operating characteristics (ROC) as a measure of detection performance are shown in Fig. 5(a) and Fig. 5(b). Based on the ROCs, the MCWC outperformed WDM and thresholding at the two tested SNR levels.

4 Cortical Neural Modifications during a Cognitive Learning Control Task

The neural events leading to a voluntary movement, or an intentional purposeful movement, may be characterized by three complex processes: target identification, plan of action, and execution. Several distinct regions of the cerebral cortex are believed to be involved in governing these processes, including the posterior parietal cortex, the premotor areas (PM) of the frontal cortex, and the primary motor cortex (M1) [Kandel et al. (2000)]. Premotor and parietal areas appear to participate in a fundamental event necessary to purposeful movement - the translation of sensory inputs into motor coordinates needed to specify precise movements [Andersen et al. (2004)]. And adaptation represented in neural firing events has been observed in motor cortical areas which correlates

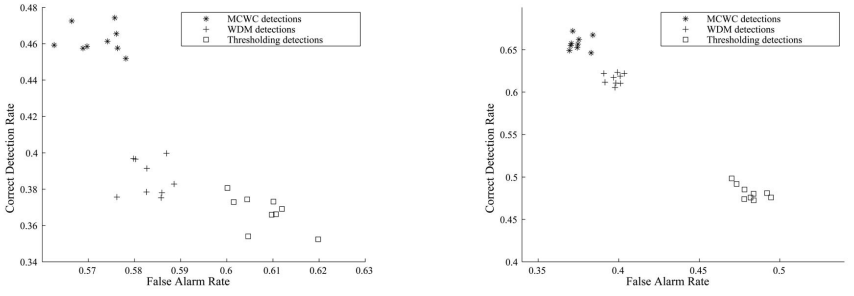

(a) Detection performance with data sets A1-1 to A1-9 (SNR=1dB)

(b) Detection performance with data sets A2-1 to A2-9 (SNR=10dB)

Fig. 5. ROC performance for MCWC, WDM and Plexon thresholding: MCWC has a better performance than WDM and Plexon thresholding in low and high SNR scenarios.

with improved behavioral parameters [Kargo et al. (2004)]. To investigate the neural mechanism of cognitive control, here we studied various aspects of cortical neural firing rates to characterize their changes as rats learned a directional paddle control task. Five rats learned to press one of two paddles (left or right) which extend at 2 seconds after the onset of a directional light cue. By trial and error, most subjects improved their behavioral accuracy to 85% or above in 5 weeks. Both primary motor (MI) and premotor (PM) cortical neurons were recorded from rat's left brain (Fig. 1(a)) during the entire course of learning.

4.1 Characterizing Cortical Neural Modifications Using Firing Rates

The rat's behavioral learning control process in our experiments was divided into 3 stages: Naive, Improving, and Stable according to the behavioral accuracy (Fig. 6(a), rat W09 for example). As it usually takes the rat several weeks to improve the accuracy to a high and stable level, the reaction time, in response to both the center ready paddle (to start a trial) and the control paddle (to control the lights), became stabilized in only a few days (Fig. 6(b)). This may indicate that it is the cognitive aspect of the behavioral task, rather than the motor skill, that the rat learned in this experiment.

Correct trials were grouped as L and R trials, representing either left or right movement directions. A task trial was sliced to form 4 epochs, which are cue on (CO), movement onset (MO), getting ready (RE) (0-400ms, 400-800ms and 1400-1800ms, respectively, after cue onset), and preparing to press (PP, 400-0ms before first press).

For MI neurons, significant mean firing rate changes ($p < 0.001$, ANOVA) through the three learning stages were observed in right (contralateral to the recording sites) but not left trials (Fig. 7). For example, the mean firing rates over the 3 stages in the CO epoch of R trials are 33.5, 36.2 and 38.5 Hz, and the mean rates of L trials in the same epoch are 37.7, 36.9 and 37.4 Hz. In PM neurons, there was statistically significant firing rate change in all epochs. The rate changes were more pronounced in the first

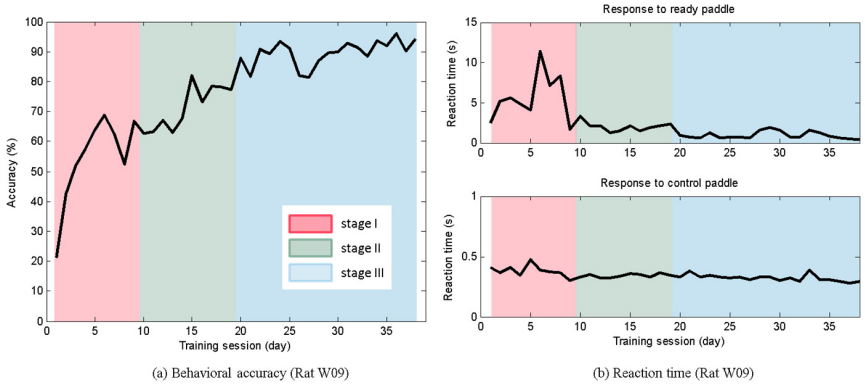

(a) Behavioral accuracy (Rat W09) (b) Reaction time (Rat W09)

Fig. 6. Behavioral results: (a) accuracy and (b) reaction time

three epochs (e.g. PM neurons R trials, CO: 41.9 ±25.1, 39.9 ±23.9, 49.0 ±22.8 Hz) than in PP (PM neurons R trials: 43.0 ±27.4, 41.0 ±25.5, 43.3 ±22.9 Hz). The PP epoch is immediately before control paddle press, which had been a familiar motor skill before the rat was recorded. But the first three epochs, during which the rat observed the cue light and made decision of movement direction, were believed to involve more cognitive effort. So the changes in mean firing rates found in the same period might be associated with the cognitive learning process.

The mean Fano factor (FF, variance over mean of trial based firing rates) value of both MI and PM neuron ensembles increased with learning (Fig. 8). Meanwhile, decrement of the standard deviation of the FF values was observed in some cases (e.g. 2.05, 1.71 and 1.53, MI neurons in L trials and RE epoch). A potential explanation for this is that single neurons increased their firing variability as a means of characterizing plasticity during the acquisition of a new task.

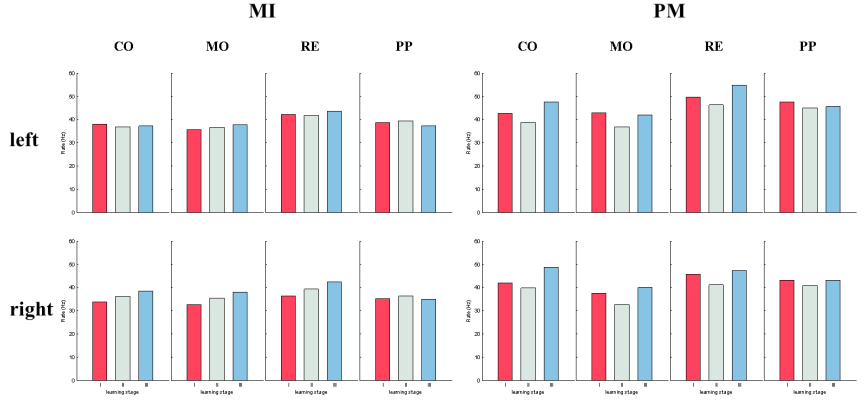

Fig. 7. Mean firing rates of the three learning stages, Naive (red), Improving (green), and Stable (blue), in four trial epochs for MI and PM neurons

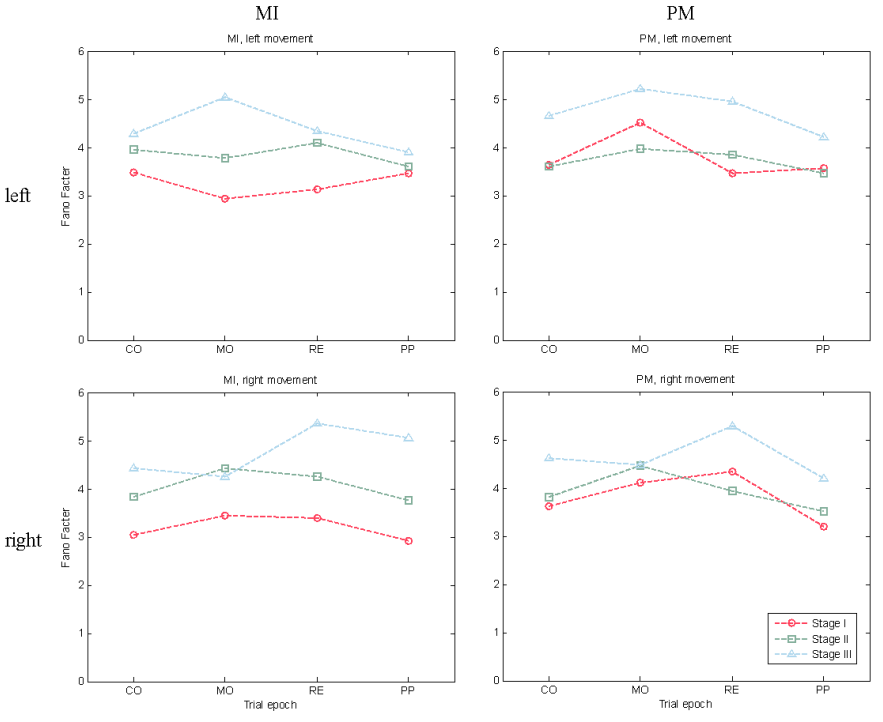

Fig. 8. Median Fano Factor value of the three learning stages, in four trial epochs for MI and PM neurons

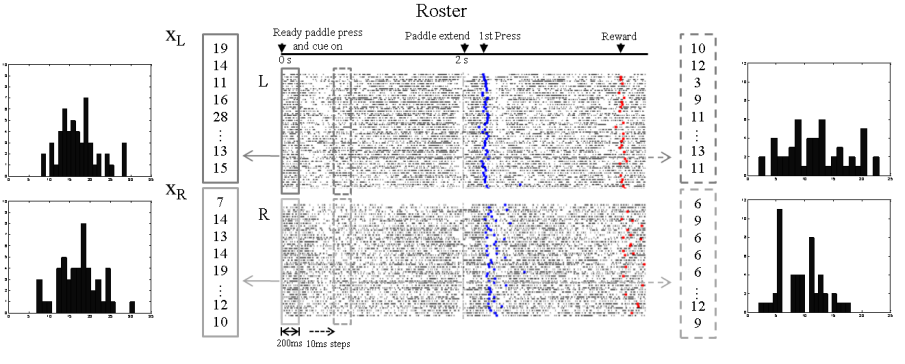

Fig. 9. An illustration of measuring statistical firing rate differences between L and R trials

The difference in firing rates between L and R trials was also measured. As shown in Fig. 9, a 200ms window was moved at 10ms steps through the trial time. The number of spikes within the window in each trial was counted and grouped for L and R trials. Mann-Whitney *U*-test was then performed to evaluate the statistical difference between

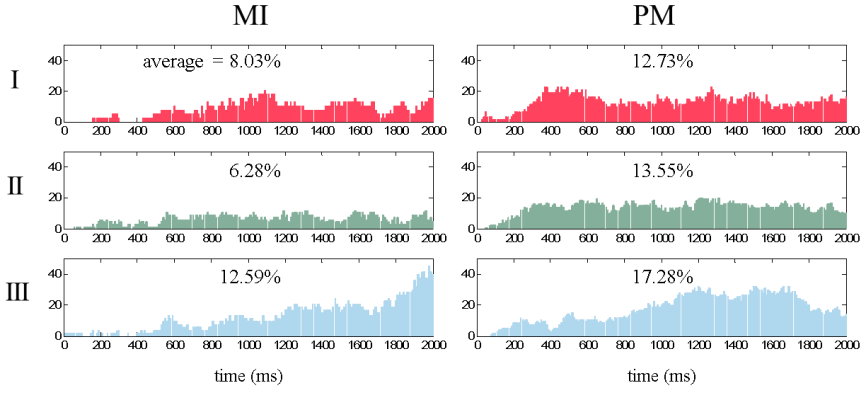

Fig. 10. The percentage of neurons showing significant difference ($P < 0.01$, Mann-Whitney U-test) in firing rates between left and right movement.

the two groups. And this was done for all neurons in all recording sessions. As a result, more PM neurons (7.5%, 8.1% and 5.7% in 3 stages) showed significant differences ($p < 0.01$, Mann-Whitney U-test) than MI neurons (1.2%, 2.5% and 1.3%) during the CO epoch (Fig. 10), when sensory information was processed and a decision of movement direction was made.

To summarize, motor cortical neural firing rate modulations were observed during the entire course of learning a cognitive control task. The mean firing rate change of motor cortical neural ensemble may be an indication of cognitive development. The increment of neuronal Fano factor value indicated that individual neurons fired more differently between trials after learning the task. A higher percentage of PM neurons responded differently in response to different cues during the preparation phase of the task, which is very likely when subjects interpreted sensory cues and planned the movement. These results suggested the followings, (1) neural adaptation may be reflected in the mean firing rate of a motor cortical neural ensemble during learning of a cognitive control task, and (2) a larger percentage of PM neurons may be involved in interpreting sensory stimuli and motor planning than M1 neurons.

4.2 Role of Motor Cortical Neurons in a Directional and Sequential Control Task

In order to examine the roles of neural coding in the primary motor cortex (M1) and the premotor cortex (PM) [Paxinos et al. (2007)] of rats during natural movement, for example cognitive control by multiple paddle presses in our experiment, we hypothesize that M1 neuronal responses change as a function of the movement context.

There is growing evidence of M1's involvement in sequential tasks using a monkey model [Ben-Shaul et al. (2004); Carpenter et al. (2004); Kakei et al. (1999); Li et al. (1999); Lu et al. (1999); Shima et al. (2000)] in memorized tasks and learning new aspects of a task [Shima et al. (2000)]. However, in a rat model, existing studies were

only based on short-duration behavioral tasks (e.g. 20ms) and therefore unable to make similar statements. Furthermore, little anatomical or functional evidence shows that rats have a pre-SMA and it is still inconclusive that rats having a mixture of ventral premotor (PMv) and SMA, and thus leaving the question open if rat's motor cortical neurons are present and encode sequential information.

In our experiment, the experiment apparatus provides five light cue positions at center (C), single left (L), and double left (LL); similarly for the right side. A rat was to press one of the two directional paddles to move the cue light to the center. As a trial started, one of the five cues was lit for the rat to respond in 2s. In response to the cue light position, the rat made a single or double presses on the paddle with each press move the light to the respective direction once. The rat worked for food rewards when he moved the light cue to the center position and kept there for 1s. Neural waveforms were recorded in the primary motor (M1) and the premotor (PM) areas while rats learned to perform this control task from a naive state to finally mastering it in about 30 sessions (days) on average.

The motor cortical neurons displayed some unique patterns. Using three-way ANOVA (direction (left or right) vs. task sequence length (single or double) vs. order (first or second)) analysis on the neural firing rates (20ms bin). 26% of M1 neurons and 26% of PM neurons were found to represent directional selectivity ($p < 0.01$ for left and right) as shown in Fig. 11, and an example raster is shown in Fig. 12(a). However, only 5% neurons showed significant difference between the L and LL trials ($p < 0.01$ for single versus double presses) when the rat responded to the cue and made his first press. Similar for R and RR trials. Among all recorded neurons, 28% of M1 neurons and 29% of PM neurons showed order selectivity ($p < 0.01$ for the L, LL 1st press versus the 2nd press in LL), as shown in Fig. 12(b). Figure 12(c) is an example of another kind of neurons, which has a tendency of both directional and sequential selectivity.

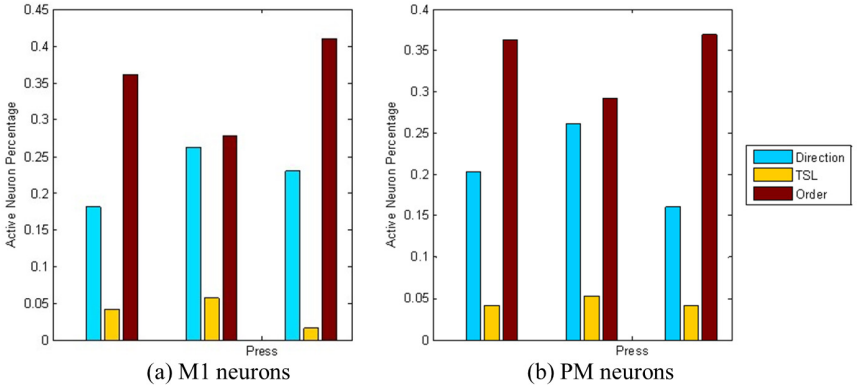

(a) M1 neurons (b) PM neurons

Fig. 11. 3-way ANOVA of M1 and PM neurons on 3 adjacent windows (length: 20ms) around press on direction (left or right), task sequence length (single or double), and order (first or second). (a) 26% of M1 neurons were found to represent directional selectivity, and 5% and 28% were task sequence length and order selective, respectively. (b) 26% of PM neurons were found to represent directional selectivity, and 6% and 29% were task sequence length and sequence selective, respectively.

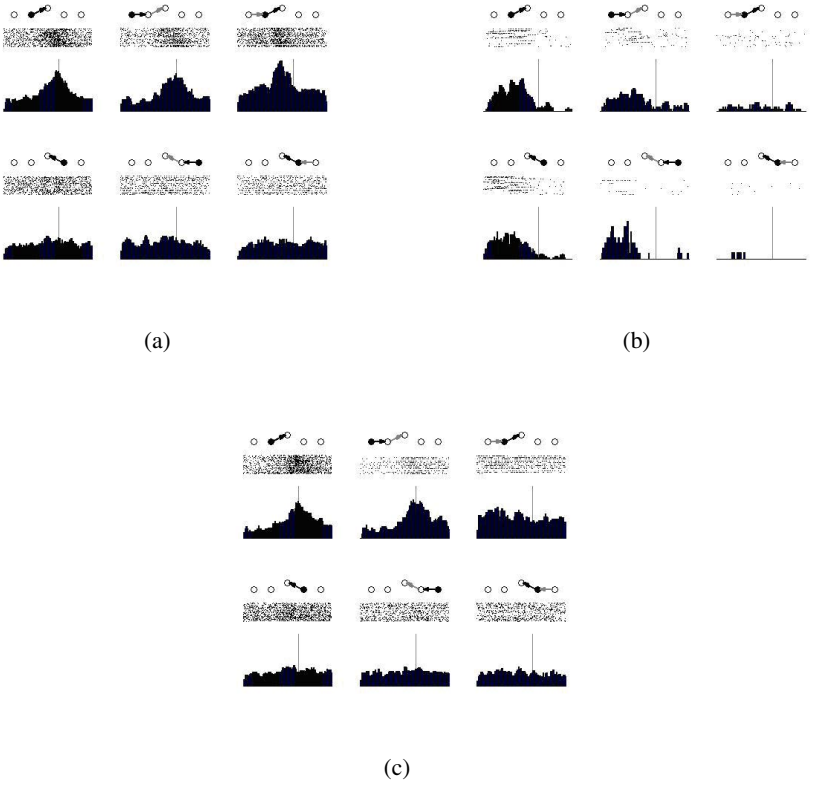

Fig. 12. (a) Raster for T10 channel 4, a M1 neuron on 1/15/2011 representing directional information. Direction sensitive. (b) Raster for T10 channel 15, a PM neuron on 12/15/2010 representing sequential information. Higher firing rates for single press and the first presses of LL and RR trials before movement onset. (c) Raster for T10 channel 4, a M1 neuron on 1/6/2011 representing directional and sequential information. Left: order sensitive; right: none.

Our results suggest that in addition to commonly believed roles for motor cortical areas, they may also be useful in storing and representing sequential movements in rats.

5 Conclusion

The ultimate goal of our studies is to unveil the neural code in relation to cognitive control behaviors. Toward this end, we made use of a rat model and recorded the rats' motor cortical areas using multiple electrode to obtain single unit recordings while the rats performed a directional control task through associative learning. We began our study by introducing a new, automated spike detection algorithm, MCWC, which makes use of correlation and comparison among continuous wavelet transform coefficients at multiple scales. This algorithm provided us the freedom to conduct analysis on large

volume of neural recordings with objective measures for spike detection and sorting. Based on this result, we were able to conduct several further analysis using spike rates to analyze spike firing patterns in association with the behavioral learning process and the many aspects of the control task, such as directional control, sequential control, and so on. We found that the role for M1 in a multiple press task is beyond that of controlling movements; the context of a movement contributes to shaping M1 representations, and that the PM is more actively involved in the learning aspect of the cognitive control task.

References

Andersen, R., Musallam, S., Pesaran, B.: Selecting the signals for a brain-machine interface. Current Opinion in Neurobiology 14, 720–726 (2004)

Bao, P., Zhang, L.: Noise reduction for magnetic resonance images via adaptive multiscale products thresholding. IEEE Transactions on Medical Imaging 22(9), 1089–1099 (2003)

Benitez, R., Nenadic, Z.: Robust Unsupervised Detection of Action Potentials With Probabilistic Models. IEEE Transactions on Biomedical Engineering 55(4), 1344–1354 (2008)

Ben-Shaul, Y., Drori, R., Asher, I., Stark, E., Nadasdy, Z., Abeles, M.: Neuronal activity in motor cortical areas reflects the sequential context of movement. J. Neurophysiol. 91, 1726–1748 (2004)

Carpenter, A., Georgopoulos, A., Pellizzer, G.: Motor cortical encoding of serial order in a context-recall task. Science 283, 1752–1757 (1999)

Dedual, N., Ozturk, M., Sanchez, J., Principe, J.: An associative memory readout in ESN for neural action potential detection. In: International Joint Conference on Neural Networks, IJCNN 2007, p. 2295 (2007)

Fee, M.S., Mitra, P.P., Kleinfeld, D.: Variability of extracellular spike waveforms of cortical neurons. Journal of Neurophysiology 76(6), 3823–3833 (1996)

Hulata, E., Segev, R., Ben-Jacob, E.: A method for spike sorting and detection based on wavelet packets and shannon's mutual information. Journal of Neuroscience Methods 117(1), 1–12 (2002)

Hulata, E., Segev, R., Shapira, Y., Benveniste, M., Ben-Jacob, E.: Detection and sorting of neural spikes using wavelet packets. Phys. Rev. Lett. 85(21), 4637–4640 (2000)

Humphrey, D., Schmidt, E.: Extracellular Single-Unit Recording Methods. Neurophysiological Techniques: Applications to Neural Systems 15, 1–64 (1991)

Kakei, S., Hoffman, D., Strick, P.: Muscle and movement representations in the primary motor cortex. Science 285, 2136–2139 (1999)

Kandel, E., Schwartz, J., Jessell, T.: Principles of Neural Science (2000)

Kargo, W., Nitz, D.: Improvements in the Signal-to-Noise Ratio of Motor Cortex Cells Distinguish Early versus Late Phases of Motor Skill Learning. J. Neurosci. 24, 5560–5569 (2004)

Kim, K.H., Kim, S.J.: A wavelet-based method for action potential detection from extracellular neural signal recording with low signal-to-noise ratio. IEEE Transactions on Biomedical Engineering 50(8), 999–1011 (2003)

Kreiter, A.K., Aertsen, A.M., Gerstein, G.L.: A low-cost single-board solution for real-time, unsupervised waveform classification of multineuron recordings. Journal of Neuroscience Methods 30(1), 59–69 (1989)

Li, C., Padoa-Schioppa, C., Bizzi, E.: Neuronal correlates of motor performance and motor learning in the primary motor cortex of monkeys adapting to an external force field. Neuron 30, 593–607 (2001)

Lu, X., Ashe, J.: Anticipatory activity in primary motor cortex codes memorized movement sequences. Neuron 45, 967–973 (2005)

Mallat, S.: A wavelet tour of signal processing. Academic Press, San Diego (1989)

Matsuzaka, Y., Picard, N., Strick, P.: Skill Representation in the Primary Motor Cortex After Long-Term Practice. J. Neurophysiol. 97, 1819–1832 (2007)

Musial, P., Baker, S., Gerstein, G., King, E., Keating, J.: Signal-to-noise ratio improvement in multiple electrode recording. Journal of Neuroscience Methods 115, 29–43 (2002)

Naundorf, B., Wolf, F., Volgushev, M.: Unique features of action potential initiation in cortical neurons. Nature 440(7087), 1060–1063 (2006)

Nenadic, Z.: Spike detection with the continuous wavelet transform, matlab software. University of California, Irvine, Center for BioMedical Signal Processing and Computation (2005), http://cbmspc.eng.uci.edu

Nenadic, Z., Burdick, J.: Spike detection using the continuous wavelet transform. IEEE Transactions on Biomedical Engineering 52(1), 74–87 (2005)

Nenadic, Z., Burdick, J.: A control algorithm for autonomous optimization of extracellular recordings. IEEE Transactions on Biomedical Engineering 53(5), 941–955 (2006)

Olson, B., Si, J., Hu, J., He, J.: Closed-loop cortical control of direction using support vector machines. IEEE Transactions on Neural Systems and Rehabilitation Engineering 13(1), 72–80 (2005)

Oweiss, K., Anderson, D.: A multiresolution generalized maximum likelihood approach for the detection of unknown transient multichannel signals in colored noise with unknown covariance. In: Proceedings of IEEE International Conference on Acoustics, Speech, and Signal Processing, ICASSP 2002, vol. 3, pp. 2993–2996 (2002)

Oweiss, K., Anderson, D.: A unified framework for advancing array signal processing technology of multichannel microprobe neural recording devices. In: 2nd Annual International IEEE-EMB Special Topic Conference on Microtechnologies in Medicine and Biology, pp. 245–250 (2002)

Paxinos, G., Watson, C.: The Rat Brain in Stereotaxic Coordinates (2007)

Quiroga, R.Q., Nadasdy, Z., Ben-Shaul, Y.: Unsupervised spike detection and sorting with wavelets and superparamagnetic clustering. Neural Computation 16(8), 1661–1687 (2004)

Sadler, B.M., Swami, A.: Analysis of multiscale products for step detection and estimation. IEEE Transactions on Information Theory 45(3), 1043–1051 (1999)

Santaniello, S., Fiengo, G., Glielmo, L., Catapano, G.: A biophysically inspired microelectrode recording-based model for the subthalamic nucleus activity in parkinson's disease. Biomedical Signal Processing and Control 3(3), 203–211 (2008)

Shima, K., Tanji, J.: Neuronal activity in the supplementary and presupplementary motor areas for temporal organization of multiple movements. J. Neurophysiol. 84, 2148–2160 (2000)

Smith, L.: Noisy spike generator, matlab software. University of Stirling, Department of Computing Science and Mathematics (2006), http://www.cs.stir.ac.uk/~lss/noisyspikes/

Song, M.J., Wang, H.: A spike sorting framework using nonparametric detection and incremental clustering. Neurocomputing 69(10-12), 1380 (2006)

Thakur, P.H., Lu, H., Hsiao, S.S., Johnson, K.O.: Automated optimal detection and classification of neural action potentials in extra-cellular recordings. Journal of Neuroscience Methods 162(1-2), 364–376 (2007)

Volgushev, M., Malyshev, A., Balaban, P., Chistiakova, M., Volgushev, S., Wolf, F.: Onset Dynamics of Action Potentials in Rat Neocortical Neurons and Identified Snail Neurons: Quantification of the Difference. PLoS ONE 3(4), e1962 (2008)

Wood, F., Black, M., Vargas-Irwin, C., Fellows, M., Donoghue, J.: On the variability of manual spike sorting. IEEE Transactions on Biomedical Engineering 51(6), 912–918 (2004)

Wu, G., Hallin, R.G., Ekedahl, R.: Multiple action potential waveforms of single units in man as signs of variability in conductivity of their myelinated fibres. Brain Research 742(1-2), 225–238 (1996)

Xu, Y., Weaver, J., Healy, D., Lu, J.: Wavelet transform domain filters: a spatially selective noise filtration technique. IEEE Transactions on Image Processing 3(6), 747–758 (1994)

Yang, C., Olson, B., Si, J.: A multiscale correlation of wavelet coefficients approach to spike detection. Neural Computation 23, 215–250 (2011)

Yang, X., Shamma, S.: A totally automated system for the detection and classification of neural spikes. IEEE Transactions on Biomedical Engineering 35(10), 806–816 (1988)